Am. J. Hum. Genet. 74:917–930, 2004

Rare Autosomal Recessive Cardiac Valvular Form of Ehlers-Danlos Syndrome Results from Mutations in the *COL1A2* Gene That Activate the Nonsense-Mediated RNA Decay Pathway

Ulrike Schwarze,[1] Ryu-Ichiro Hata,[3] Victor A. McKusick,[4] Hiroshi Shinkai,[5] H. Eugene Hoyme,[6] Reed E. Pyeritz,[7] and Peter H. Byers[1,2]

Departments of [1]Pathology and [2]Medicine, University of Washington, Seattle; [3]Department of Biochemistry and Molecular Biology and Research Center of Advanced Technology for Craniomandibular Function, Kanagawa Dental College, Yokosuka, Japan; [4]McKusick-Nathans Institute of Genetic Medicine, Baltimore; [5]Department of Dermatology, Chiba University School of Medicine, Chiba, Japan; [6]Department of Pediatrics, Stanford University School of Medicine, Stanford; and [7]Department of Medicine, University of Pennsylvania, Philadelphia

Splice site mutations in the *COL1A2* gene of type I collagen can give rise to forms of Ehlers-Danlos syndrome (EDS) because of partial or complete skipping of exon 6, as well as to mild, moderate, or lethal forms of osteogenesis imperfecta as a consequence of skipping of other exons. We identified three unrelated individuals with a rare recessively inherited form of EDS (characterized by joint hypermobility, skin hyperextensibility, and cardiac valvular defects); in two of them, *COL1A2* messenger RNA (mRNA) instability results from compound heterozygosity for splice site mutations in the *COL1A2* gene, and, in the third, it results from homozygosity for a nonsense codon. The splice site mutations led to use of cryptic splice donor sites, creation of a downstream premature termination codon, and extremely unstable mRNA. In the wild-type allele, the two introns (IVS11 and IVS24) in which these mutations occurred were usually spliced slowly in relation to their respective immediate upstream introns. In the mutant alleles, the upstream intron was removed, so that exon skipping could not occur. In the context of the mutation in IVS24, computer-generated folding of a short stretch of mRNA surrounding the mutation site demonstrated realignment of the relationships between the donor and acceptor sites that could facilitate use of a cryptic donor site. These findings suggest that the order of intron removal is an important variable in prediction of mutation outcome at splice sites and that folding of the nascent mRNA could be one element that contributes to determination of order of splicing. The complete absence of proα2(I) chains has the surprising effect of producing cardiac valvular disease without bone involvement.

Introduction

Classic Ehlers-Danlos syndrome (EDS) (MIM 130000 and MIM 130010), also known as "EDS types I and II," is generally a dominantly inherited condition characterized by joint laxity, skin hyperextensibility and friability, and abnormal scar formation. It usually results from mutations in the *COL5A1* gene (Nicholls et al. 1996; Wenstrup et al. 1996, 2000; De Paepe et al. 1997; Giunta and Steinmann 2000; Schwarze et al. 2000; Bouma et al. 2001). Mutations in the *COL5A2* gene (Michalickova et al. 1998; Richards et al. 1998), the tenascin X gene (*TNXB* [MIM 606408]) (Burch et al. 1997; Schalkwijk et al. 2001), and the gene that encodes the proα1(I) chains of type I procollagen (*COL1A1*) (Nuytinck et al. 2000) have also been implicated.

A recessively inherited form of EDS characterized by the changes of classic EDS results from failure to synthesize proα2(I) chains of type I procollagen (MIM 120160) (Sasaki et al. 1987; Hata et al. 1988). In addition to the usual skin and joint involvement, individuals with this form of EDS appear to be at increased risk for cardiac valvular dysfunction. In one instance in which homozygosity for a *COL1A2* splice site mutation (IVS46+2T→C) was identified (Nicholls et al. 2001), although no proα2(I) chains could be seen, the patient had a mixed phenotype that included elements of osteogenesis imperfecta (OI)—skull and long-bone fractures—but there was no cardiovascular system involvement by age 9 years.

We have now identified causative mutations in the *COL1A2* gene in three unrelated individuals whose skin fibroblasts failed to make proα2(I) chains and who had EDS and cardiovascular involvement but no suggestion of OI. Each individual either was a compound heterozygote for two splice mutations that led to mRNA in-

Received December 19, 2003; accepted for publication February 25, 2004; electronically published April 9, 2004.

Address for correspondence and reprints: Dr. Peter H. Byers, Department of Pathology, Box 357470, University of Washington, Seattle, WA 98195-7470. E-mail: pbyers@u.washington.edu

0002-9297/2004/7405-0013$15.00

stability in the spliced product or had a homozygous nonsense mutation.

Most splice site mutations in the *COL1A2* gene identified to date produce exon skipping and result in an OI phenotype (Byers and Cole 2002). In contrast, the splice site mutations in the form of EDS we describe here led to use of cryptic splice sites, creation of premature termination codons (PTCs), and unstable mRNAs. A nonsense mutation that introduces a PTC has the same phenotypic effect and alters mRNA processing in an identical fashion. The outcomes of the splice site mutations could be predicted by the local order of intron removal and the presence of available cryptic splice sites. These findings suggest that the order of intron removal is a critical factor in the determination of outcome of splice site mutations, which then mediates the clinical phenotypes. Further, homozygosity or compound heterozygosity for *COL1A2* null mutations appears to define a subset of individuals with EDS who have a cardiac valvular phenotype.

Patients, Material, and Methods

Patients

The three individuals described here received diagnoses, on clinical grounds, of the classic form of EDS (types I and II) and were studied further when it was noted that their cultured fibroblasts appeared to synthesize no proα2(I) chains of type I procollagen. All biopsies were performed after appropriate consent was received.

Patient 1 (P1) was a 45-year-old man who received the diagnosis of EDS type II because of recurrent shoulder dislocations since childhood, small-joint hypermobility, pectus excavatum, muscle and tendon tears, bilateral inguinal hernias, small scars under the chin and on the forehead, atrophic scars over the knees and shins, easy bruisability, and generally hyperextensible and thin skin. He was myopic and had bilateral astigmatism. For many years, he was known to have a systolic murmur, and a recent echocardiogram demonstrated anterior mitral leaflet prolapse, resulting in severe mitral regurgitation with systolic flow reversal in the left upper pulmonary vein. The left atrium and the left ventricle were dilated, there was mild ventricular hypertrophy, and there was moderate aortic insufficiency. The aortic root diameter was 36 mm (normal range 20–37 mm). Following episodes of arrhythmias and atrial fibrillation, he underwent mitral and aortic valve replacement surgery. The procedure itself was uneventful; however, once the prosthetic valves were placed, first the mitral annulus (not the prosthetic valve) dehisced from the ventricle, then the aortic valve separated from the atrioventricular groove, and finally there was massive leakage through the left ventricular myocardium with disintegration of the entire left ventricle, from which the patient died.

The subject's mother and his only child have mild joint laxity without dislocations. Collagen fibrils in skin were slightly larger than normal and more ovoid than in control individuals but did not contain the characteristic aggregate fibrils seen in skin from individuals with EDS type I (Vogel et al. 1979).

Patient 2 (P2) is a woman with EDS type II, described elsewhere (Kojima et al. 1988), who is now aged 65 years. She was reported to have soft skin, moderate skin hyperextensibility, joint hypermobility (especially of the fingers and hands), easy bruisability, and atrophic scar formation. At age 38 years, she sought evaluation because of palpitations, a pansystolic murmur, dyspnea, and fatigue, which led to the diagnosis of mitral valve insufficiency. Mitral valve replacement surgery was performed, and the postoperative course was largely uneventful.

Collagen fibrils in skin showed more variation in diameter than normal, but composite fibrils were not detected (Kojima et al. 1988).

P2 has no history of fractures. Her skin hyperextensibility and joint hypermobility have remained unchanged. She has no children.

Patient 3 (P3) is a 30-year-old man whose phenotypically normal parents are second cousins. He was born with bilateral inguinal hernias and, as a teenager, underwent surgical repair of pes planus and calcaneovalgus. He has always had significant large- and small-joint hypermobility, with bilateral genu recurvatum. His skin is soft and hyperextensible, with striae at the lateral aspect of the abdomen. He bruises easily, and his wound healing is delayed. He had a large secundum-type atrial septal defect, mitral valve prolapse with significant mitral regurgitation, and severe aortic valve regurgitation. His aortic root diameter at age 29 years was 36 mm, at the upper limit of normal. He developed marked left ventricular enlargement and had his aortic and mitral valves replaced with prosthetic valves, with no surgical complications. Of note, the femoral artery and vein perforated in the course of preoperative diagnostic cardiac catheterization, and the cardiac surgeon described his tissues as extremely soft. P3 has a 27-year-old brother, with hyperextensible small joints and soft but not significantly hyperextensible skin, who required aortic valve replacement at age 25 years because of aortic insufficiency. Their parents are reported to have no evidence of valvular heart disease.

Cell Culture and Analysis of Collagenous Proteins

Dermal fibroblasts were obtained from explants of skin biopsies from the three individuals. Growth and maintenance of those and control cell strains, radiola-

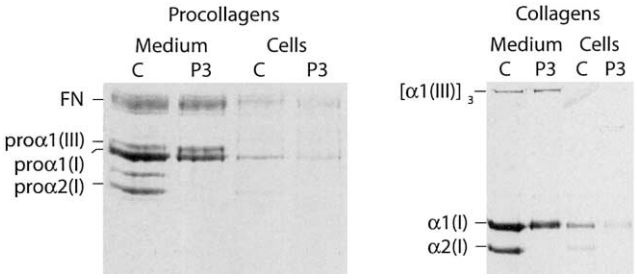

Figure 1 SDS-PAGE of radiolabeled procollagens and collagens. Procollagens were analyzed under reducing conditions, whereas collagens were separated without prior reduction. In P3, proα2(I) and α2(I) chains were absent, and some overmodification due to the formation of proα1(I) homotrimers was visible as a slight delay in electrophoretic mobility of the α1(I) chains. Cells from the other two patients behaved in the same manner. FN = fibronectin.

beling of collagenous proteins, and analysis of proα chains and α chains with SDS-PAGE were performed as described elsewhere (Bonadio et al. 1985).

Preparation of cDNA and Genomic DNA

Total cellular RNA and genomic DNA were extracted, using the RNeasy Mini Kit (Qiagen) and QIAamp DNA Mini Kit (Qiagen), respectively, from cultured dermal fibroblasts of the patients and a control individual. In addition, nuclear RNA was prepared from cultured fibroblasts of P1 and a control cell strain by use of reagents from the RNeasy Mini Kit. In brief, confluent 100-mm plates were rinsed with ice cold 1X PBS before the addition of 500 μl of ice-cold RLN-buffer (50 mM Tris-Cl, pH 8.0; 140 mM NaCl; 1.5 mM $MgCl_2$; 0.5% [v/v] Nonidet P-40). The cells were gently detached with a sterile cell scraper, were transferred to a microfuge tube, and were incubated on ice for 5 min to lyse the plasma membrane. Following centrifugation (5 min; 700 × *g;* 4°C), there was a soft, translucent pellet that contained the nuclei and the supernatant that contained the cytoplasmic fraction. The latter was carefully transferred to a new tube, 600 μl of Qiagen's RLT-buffer with β-mercaptoethanol (β-ME) was added, and the mixture was stored at −80°C for later isolation of the cytoplasmic RNA, according to the manufacturer protocol. To remove residual cytoplasmic RNA from the nuclear fraction, 300 μl of RLN-buffer was added, and, after centrifugation (3 min; 700 × *g;* 4°C), the supernatant was discarded. Then 700 μl of RLT-buffer with β-ME was added, and the genomic DNA was sheared by repeated passage through a 22G needle. After centrifugation (5 min; 21,000 × *g;* 20°C), the supernatant was transferred to a new microfuge tube, 700 μl of 70% ethanol was added, and the RNA was isolated using the RNeasy column, as described by the manufacturer. The RNA was eluted from the column in 70 μl of DEPC-water.

cDNA was synthesized by priming total RNA with random hexamers in the presence of Superscript II reverse transcriptase (Invitrogen) or priming nuclear RNA after treatment with DNase I (Roche) for 20 min at 37°C, with the incubation buffer recommended by the manufacturer. To check for residual genomic DNA in the RNA preparation, a control PCR was done without prior reverse transcription.

Amplification of the COL1A2 *Coding Sequence and Sequence Determination of Aberrant Products*

The *COL1A2* cDNA was amplified in five overlapping fragments, with primer sets listed in table A (online

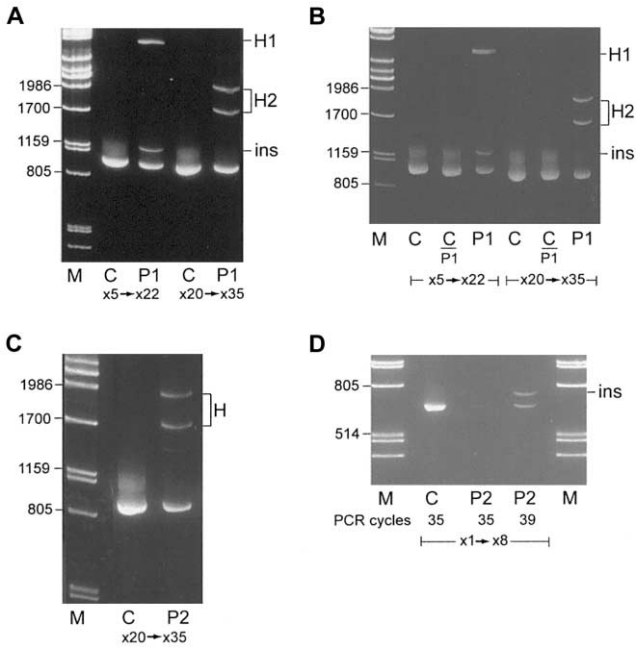

Figure 2 Amplification of *COL1A2* coding sequence. *A,* Amplification products extending from exon 5 to 22 and from exon 20 to 35 in a control individual (C) and in P1. In P1, in addition to the normal-size band, there were a slower-than-normal migrating band (ins) and a heteroduplex band (H1) in the x5→x22 product and a pair of heteroduplex bands (H2) in the x20→x35 product. *B,* Very low abundance of mutant transcripts in P1. The same PCRs were performed as for panel A, but when a C/P1 cDNA-mix was used as PCR template, only normal transcripts from the control individual were visible, indicating that transcripts from both *COL1A2* alleles in P1 were of very low abundance. *C,* Amplification products extending from exon 20 to 35 in the control individual and P2. The pair of heteroduplex bands in P2 (H) looked identical to that seen in P1. *D,* Amplification products extending from exon 1 to 8 in the control individual and P2. Owing to poor P2 cell growth, the RNA preparation was of low concentration, and, after 35 PCR cycles, there was hardly any product visible. It required 39 cycles to visualize the two products, one of normal size and a second one of slower mobility (ins). M = λ × *Pst*I (molecular size marker).

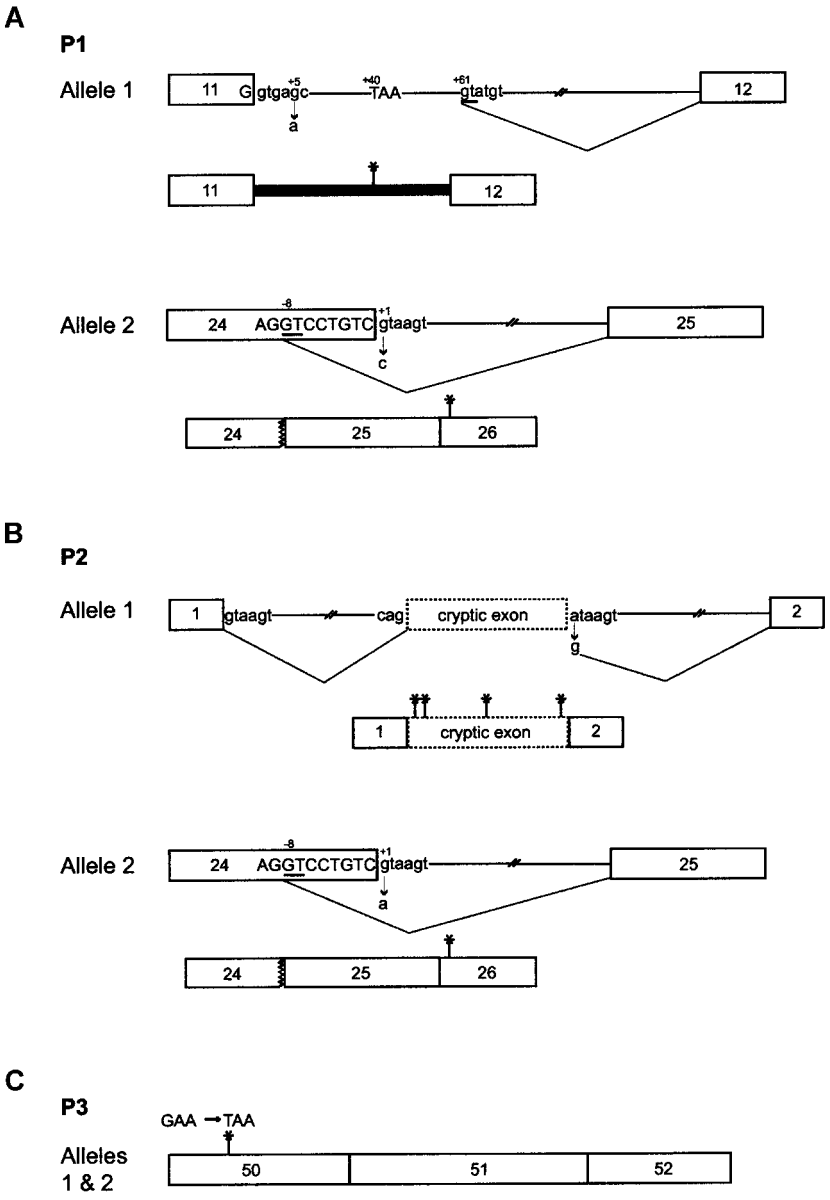

Figure 3 Schematic depiction of the "null" mutations identified in both *COL1A2* alleles in each of the three patients. Asterisks (*) indicate the locations of in-frame PTCs. *A,* In P1, one allele, IVS11+5G→A, resulted in use of a cryptic donor site 61 nt downstream (*underlined*) and inclusion of the most-5′ 60 nt of intron 11. The mature mRNA contained an in-frame PTC. In the other allele, IVS24+1G→C resulted in use of a cryptic donor site 8 nt upstream in exon 24 (*underlined*), truncation of exon 24 by 8 nt, and a reading-frameshift with introduction of a PTC in exon 26. *B,* In P2, one allele harbored an A→G transition in intron 1 (IVS1+717A→G) that activated a cryptic exon and led to inclusion of a 105-nt exon that contained four in-frame PTCs. In the other allele, IVS24+1G→A resulted, as in P1, in use of a cryptic donor site 8 nt upstream in exon 24 (*underlined*), truncation of exon 24 by 8 nt, and a reading-frameshift with introduction of a PTC in exon 26. *C,* P3 was homozygous for a point mutation (c.3601G→T) in exon 50 that resulted in substitution of a codon for glutamic acid by a nonsense codon (E1201X).

only), and the fragments were separated on 6% nondenaturing polyacrylamide gels. If extra bands (heteroduplex and/or homoduplex bands) were present in cDNA amplification products, they were excised from the gel and reamplified, and the sequence of the reamplification products was determined by ABI PRISM BigDye Terminator cycle sequencing reaction on an ABI PRISM 310 Genetic Analyzer (Perkin-Elmer Applied Biosystems). If no aberrant amplification products were detectable, all five cDNA fragments were sequenced directly. In instances of altered pre-mRNA splicing, genomic DNA was amplified using the primer sets listed

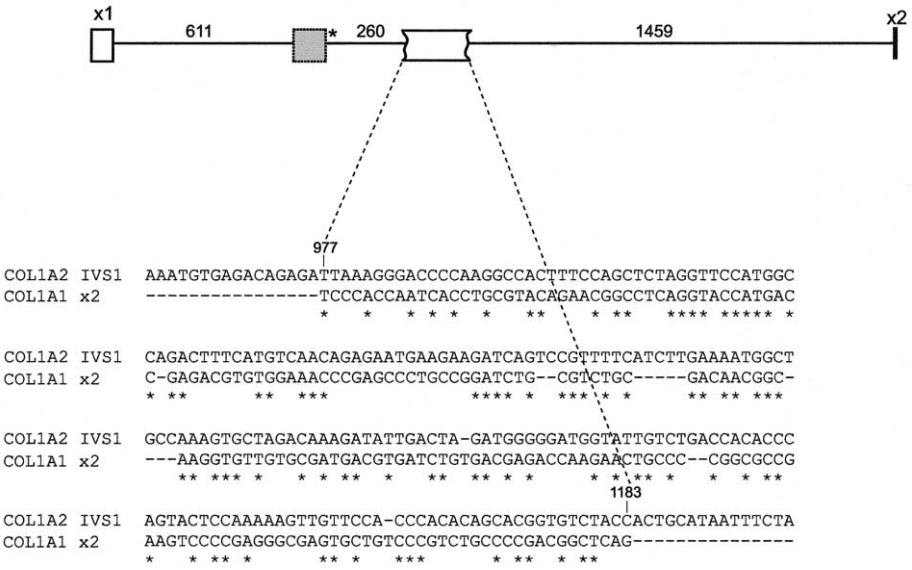

Figure 4 Relationship between the cryptic exon in *COL1A2* intron 1 and a remnant of a large exon 2 in the same domain. In one allele from P2, an A→G transition at position 717 in intron 1 (indicated by an asterisk [*]) creates a new donor site and allows inclusion of the newly defined exon (*gray box*) in the transcript. Exon 2 in the *COL1A2* gene is very small (11 nt), compared with 195 nt in the *COL1A1* gene and 203 nt in the *COL3A1* gene. This difference accounts for most of the size difference in the N-terminal propeptide. Comparison of the *COL1A1* exon 2 with the sequence of intron 1 of *COL1A2* revealed a region of 46% identity over a 207-nt interval (977–1183) of the intron, downstream from the activated cryptic exon. This suggests that the activated exon, which has no significant identity with the *COL1A1* exon 2, is not the remnant of the lost exon 2 sequences.

in table B (online only), and the products were sequenced directly to identify the causative mutation.

For P1, an additional primer pair for amplification of cDNA was used to verify that the mutations were located on separate *COL1A2* alleles. The sense primer (5′-CTTTACTCAGAAGAGAGAAAATGCCTAT-3′) was derived from the retained portion of intron 11 sequence, and the antisense primer (5′-CAGGCTCTCCTCTTGCTCCAG-3′) from exon 25.

Determination of the Order of Intron Removal in Two Regions of the COL1A2 *Gene*

To determine the order of intron removal between exon 10 and intron 12 and between exons 23 and 26 of *COL1A2* pre-mRNA, the splicing intermediates in the nucleus were analyzed by a PCR strategy described by Kessler and colleagues (1993) and detailed by Schwarze and colleagues (1999). Nucleotide sequences of the primers used are listed in table C (online only).

RNA Secondary Structure Prediction

COL1A2 sequences were folded with the RNA-folding program mfold, version 3.1 (Zuker 2003). The sequences contained exons 23–26, with introns 24 and 25 for the normal control, and exons 23–26, with intron 24 for the normal control, as well as for P1 and P2, in whom the intron 24 splice donor site was disrupted by a point mutation (see the "Results" section).

Results

Mutation Identification and Characterization

The cells from P1, P2, and P3 synthesized no detectable amounts of the proα2(I) chain of type I procollagen (fig. 1). Amplification of *COL1A2* cDNA derived from total cellular RNA yielded products detectable by PAGE for all three subjects, after 35 cycles (P1 and P3) or 39 cycles (P2) of PCR. In P1, the cDNA fragment amplified by primers in exons 5 and 22 showed, in addition to the product of normal size, a smaller amount of a more slowly migrating product and a heteroduplex band (fig. 2*A*). The overlapping fragment amplified by primers in exons 20 and 35 revealed a pair of heteroduplex bands (fig. 2*A*) and the normally sized fragment. This latter abnormality was also seen in P2 (fig. 2*C*) with the same primer pair; in addition, the fragment amplified by primers in exon 1 and 8 from P2 contained an extra band of slower-than-normal mobility (fig. 2*D*). In P3, all five overlapping cDNA fragments were of the expected size, without evidence of heteroduplex formation (not shown).

The amount of the transcripts from the mutant alleles was extremely low, as demonstrated when approxi-

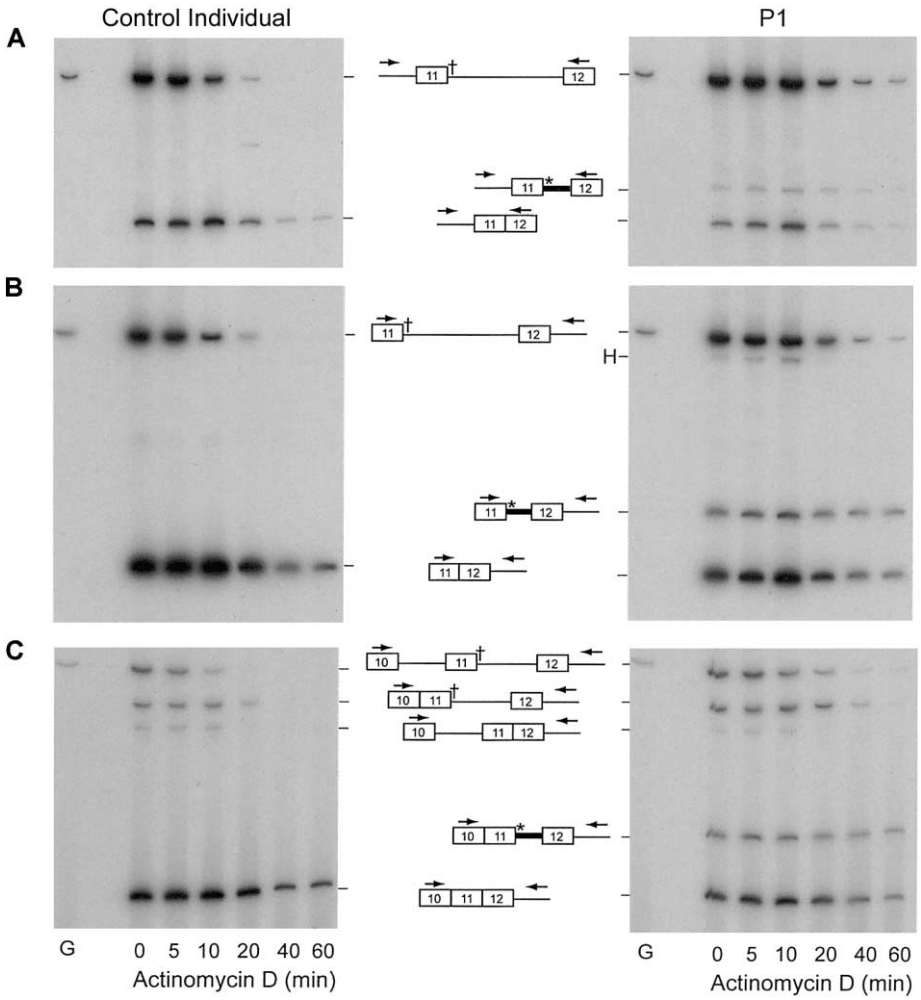

Figure 5 Order of intron removal between exon 10 and intron 12. Nuclear RNA was prepared from cultured fibroblasts after defined intervals of exposure to Actinomycin D, was treated with RNase-free DNase, was reverse transcribed, and was amplified with intron-exon primer pairs (the sense primer of which was radioactively end-labeled), and the products were separated by PAGE. The splicing intermediates, visualized by autoradiography, are schematically depicted in the center. *A, Control Individual,* The majority of the amplified product at 0 min contained introns 10 and 11; the less abundant product contained only intron 10. There was some transfer of the label from the large to the small fragment between 0 min and 10 min, but most of the label from the large fragment was lost without transfer. These findings are consistent with parallel pathways in which either intron 10 or intron 11 is removed first (fig. 6). *P1,* There is accumulation of the product that contains both intron 10 and intron 11, largely from the mutant allele. Use of a cryptic donor site in intron 11 generated a new splice intermediate, with retention of the first 60 nt (*thick black line*) in a minority of intron 10–containing transcripts. *B, Control Individual,* Intron 12 was removed slowly relative to intron 11. *P1,* There was delay of mutant allele processing, but processing of the normal allele was parallel to that in the control individual. Exon 11 of the mutant allele was "redefined" using the intronic cryptic donor site and retention of 60 nt of intron 11. The spliced mutant transcript was retained in the nucleus for a longer period than the normally spliced transcript. H = heteroduplex formed between the normally spliced product and the product that retained part of intron 11. *C, Control Individual,* Removal of intron 12 was preceded by removal of introns 10 and 11. *P1,* The processing of the mutant allele was delayed, removal of introns 10 and 11 was slower than in the control individual, and the final product of the mutant allele contained the redefined exon 11 (fig. 6). Arrows indicate the annealing sites of the amplification primers (table C [online only]). G indicates a PCR control with genomic DNA in each panel. A dagger (†) indicates the contribution in P1 of both alleles to the detected product; an asterisk (*) tags products derived from only the mutant allele (IVS11+5G→A).

mately equal amounts of control cDNA and P1 cDNA were mixed, amplified with the relevant primers, and the products examined by PAGE. None of the heteroduplexes seen when P1 cDNA alone was used as a substrate were visible (fig. 2*B*).

Compound heterozygosity in P1.—The larger fragment derived from the exon 5–22 domain in P1 (fig. 2*A* ["ins"]) included the most-5′ 60 nt of intron 11 in the mature mRNA. The included sequence contained a G→A transition at the +5 position of the intron 11 splice-donor site (IVS11+5G→A). This mutation was heterozygous in genomic DNA. In the product of that allele,

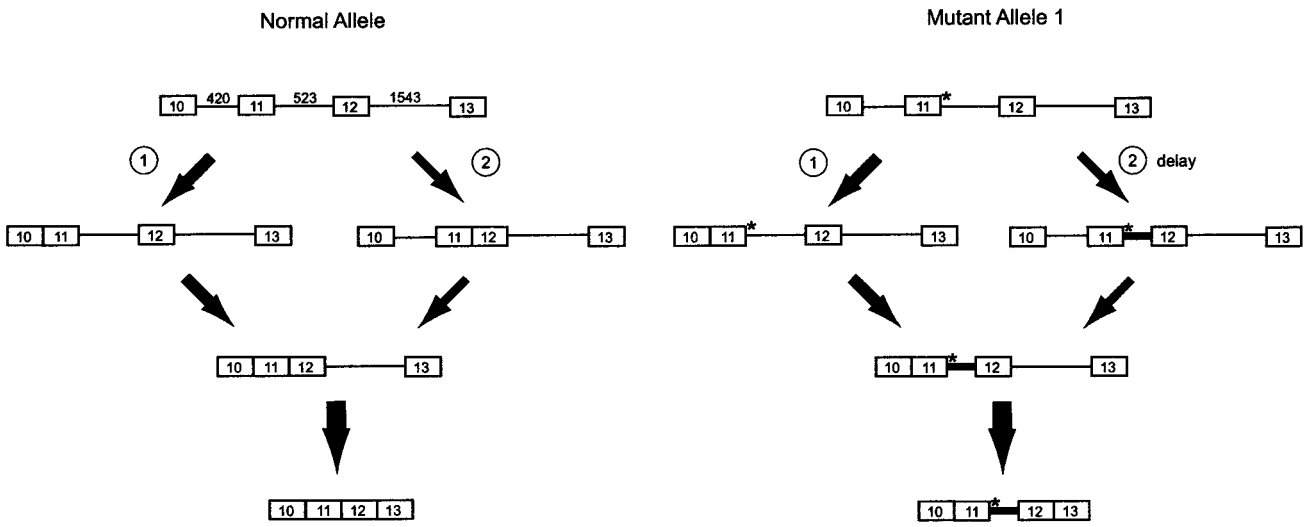

Figure 6 Pathways of removal of introns 10, 11, and 12 from the normal and mutant *COL1A2* transcripts. *Normal Allele,* Two pathways were present, a dominant one in which intron 10 was excised prior to removal of introns 11 and 12 (*encircled 1*), and a second in which removal of intron 11 preceded that of introns 10 and 12 (*encircled 2*). Intron 12 was removed last. *Mutant Allele 1,* There was delay in removal of introns 10 and 11. The intermediate was then generally processed by removal of intron 10, although in some but fewer transcripts, exon 11 was redefined using the cryptic intron 11 donor site prior to removal of intron 10 (shown in fig. 5*A*). Intron sizes are shown in the unspliced normal transcript. An asterisk (*) indicates the site of the mutation. The width of the arrows reflects the amount of product derived from the respective branch of the pathway.

a cryptic donor site 61 nt downstream in intron 11 (fig. 3*A* [*Allele 1*]) was used. The retained portion of intron 11 contained an in-frame PTC (TAA) that renders transcripts from that allele unstable due to nonsense-mediated mRNA decay (Maquat and Carmichael 2001).

Reamplification of the excised heteroduplex band seen in the same fragment (fig. 2*A* [H1]) reproduced the product pattern observed after the initial PCR (not shown), and there was no evidence of a skipped-exon product.

Sequencing of the excised and reamplified heteroduplex bands seen in P1 in the fragment extending from exon 20 to 35 (fig. 2*A* [H2]) revealed heterozygosity for truncation of exon 24 by 8 nt. Heterozygosity for a G→C transversion at the +1 position of the intron 24 splice donor site (IVS24+1G→C) led to use of a cryptic donor site 8 nt upstream in exon 24 (fig. 3*A* [*Allele 2*]). The deletion of 8 nt caused a reading-frameshift and introduced a PTC (TGA) 101 nt downstream in exon 26. To verify that the two splice donor site mutations were located on separate *COL1A2* alleles, cDNA was amplified with a sense primer that annealed to the retained portion of intron 11 and with an antisense primer in exon 25 (see the "Material and Methods" section). The presence of an intact exon 24 in this product proved that the mutations arose on separate alleles.

Compound heterozygosity in P2.—The abnormal product seen in the fragment extending from exon 1 to exon 8 (fig. 2*D* [ins]) was caused by retention of 105 nt from within intron 1 in one *COL1A2* allele comprising nt 612–716 of the intron (fig. 3*B* [*Allele 1*]). This insertion represents a cryptic exon that was flanked by a canonical splice acceptor site (cag), with an intact polypyrimidine tract and branchpoint site but an inactive splice-donor site (**a**taagt). An A→G transition created a functional donor splice site (**g**taagt [the bold nt showing the substitution]). The inserted cryptic exon contained four in-frame PTCs that led to transcript instability.

The proα2(I) chain of type I procollagen contains an amino-terminal propeptide that is substantially shorter than the homologous region in the related fibrillar collagen genes, *COL1A1* and *COL3A1*. The domain is encoded by 6 exons in *COL1A1* and *COL1A2*, but in the latter, exon 2 contains only 11 nt and exon 3 is truncated. The newly activated exon in P2 is upstream of a portion of the intron that contains a sequence similar to that seen in exon 2 of the *COL1A1* gene and that could be remnants of the ancestral gene in *COL1A2* (fig. 4).

The second abnormality detected in P2 was in the product extending from exon 20 to exon 35 and appeared to be identical, with PAGE (fig. 2*C*), to the one detected in P1 (fig. 2*A*). Sequencing revealed 3′ truncation of exon 24 by 8 nt but, in this instance, caused by a G→A transition at the +1 position of the intron 24 splice-donor site (IVS24+1G→A) in one allele that resulted in use of the same cryptic donor site in exon 24 as seen in P1 (fig. 3*B* [*Allele 2*]).

Homozygosity in P3.—A homozygous point mutation

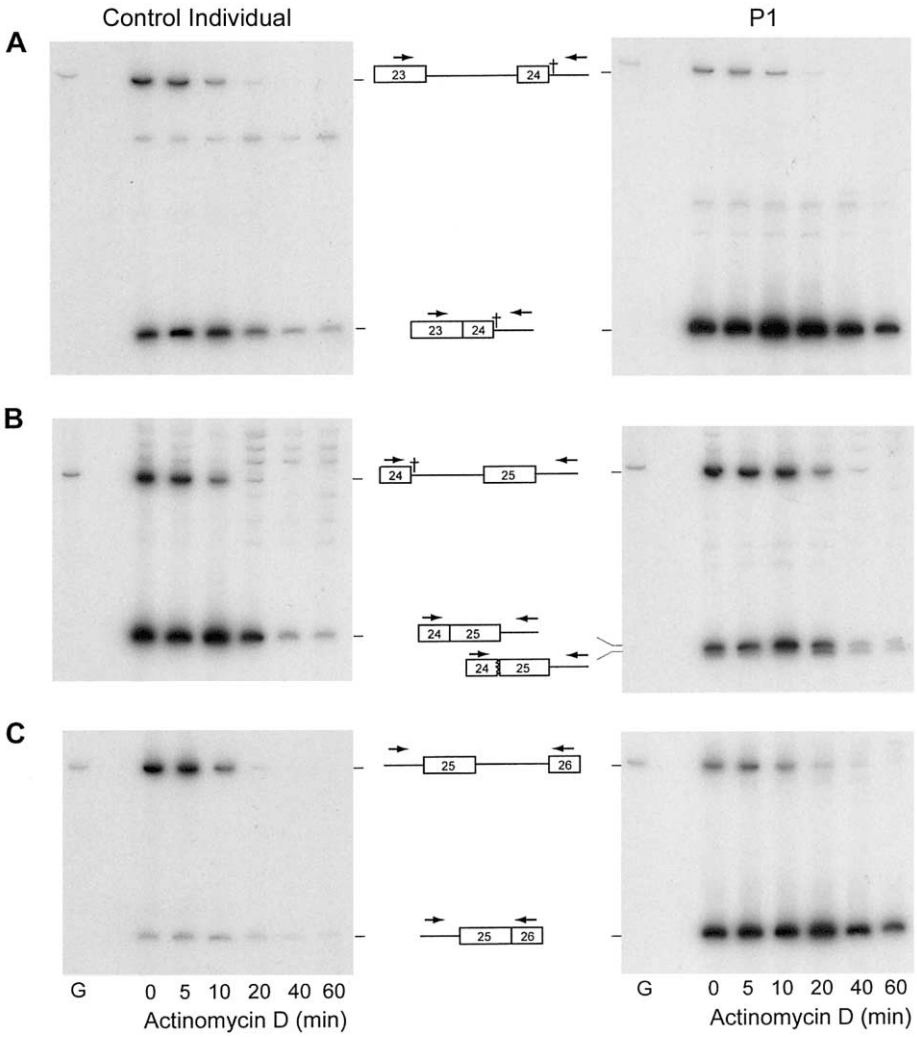

Figure 7 Order of intron removal between exons 23 and 26. The display of the data and the symbols used are identical to those in figure 5. *A, Control Individual,* Intron 23 was excised prior to intron 24 in most transcripts. *P1,* There was a major product from which intron 23 had been removed, but this product was significantly more abundant than in the control individual at all time points, as a result of stagnation of mutant transcripts prior to excision of intron 24 (fig. 8). *B, Control Individual,* Intron 24 was excised prior to intron 25 in most transcripts. *P1,* In a very small number of mutant transcripts, the removal of introns 24 and 25 followed the order that represented the dominant pathway in the control—that is, removal of intron 24 before intron 25, and generation of a shorter-than-normal splice product due to use of the cryptic exon 24 donor site that resulted in exon 24 truncation (*undulated vertical line*). *C, Control Individual,* There was hardly any signal representing a product from which intron 25 had been excised prior to excision of intron 24. *P1,* The presence of the intron 24 splice donor site mutation nearly abolished the ability to remove intron 24 prior to intron 25, and a new pathway was detected in which intron 25 was removed prior to intron 24 (fig. 8).

(c.3601G→T) in exon 50 of *COL1A2* (fig. 3C) resulted in substitution of a nonsense codon for glutamic acid (E1201X). Evidence that transcripts from those mutant alleles were very unstable was obtained from detection of only a normal sequence when cDNA from a control individual and from P3 were mixed in equal proportion before sequence template amplification (not shown). DNA from the brother of P3 was also sequenced, and the same homozygous nucleotide substitution was identified.

Determination of the Order of Intron Removal in P1 in Regions of Splice Site Mutations

Cells from P1 and from a control individual were incubated with Actinomycin D to halt transcription, and nuclear RNA was harvested after 0, 5, 10, 20, 40, and 60 min and was reverse transcribed to cDNA. Paired intron/exon primers were used to amplify different regions between exon 10 and intron 12 and

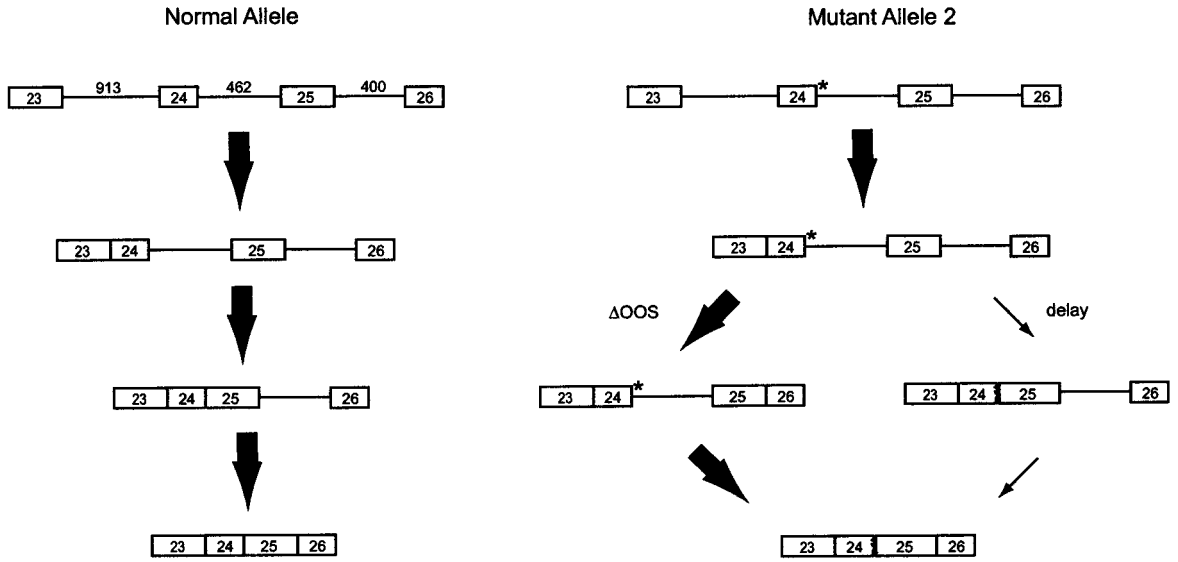

Figure 8 Pathways of removal of introns 23, 24, and 25 from normal and mutant *COL1A2* transcripts. *Normal Allele,* In the predominant splice pathway, intron 23 removal preceded the removal of intron 24, and intron 25 was removed last. *Mutant Allele 2,* As in the normal transcript, intron 23 was removed prior to removal of introns 24 and 25. The presence of the mutation significantly diminished the ability to remove intron 24 (via use of the cryptic exon 24–donor site) prior to removal of intron 25, resulting in prolonged presence of the precursor splice intermediate (shown in fig. 7) and in preferential removal of intron 25 prior to intron 24 (ΔOOS = change in order of splicing), a pathway that was barely detectable in normal transcripts. Intron sizes are shown in the unspliced normal transcripts. An asterisk (*) indicates the site of the mutation. The width of the arrows roughly reflects the amount of product derived from the respective branch of the pathway.

between exons 23 and 26 in the unspliced or partially spliced precursor mRNA.

For the control individual, when primers were placed in intron 10 and exon 12 (fig. 5*A*), the majority of the amplified product at 0 min contained intron 10 and intron 11, and a less abundant product contained only intron 10. There was some transfer of the label from the large to the small fragment between 0 min and 10 min, and the larger product diminished in intensity. These findings are consistent with parallel pathways, a dominant one in which removal of intron 10 precedes that of intron 11 and a second in which removal of intron 11 occurs prior to that of intron 10 (fig. 6).

In cells from P1 (IVS11+5G→A), the commitment of transcripts from both alleles to the two pathways appeared to be similar, but the flow of the mutant transcript through the "intron-11-before-intron-10" pathway was delayed (figs. 5 and 6), so that the product with both introns accumulated. In this pathway, the removal of intron 10 appeared to be dependent on the prior removal of intron 11. When primers in exon 11 and intron 12 (fig. 5*B*) or in exon 10 and intron 12 (fig. 5*C*) were used, it was apparent that intron 12 was very slowly removed, relative to introns 10 and 11. Products obtained with both primer sets showed a delay of mutant allele processing that appeared to be resolved by use of a cryptic donor site in intron 11. Once the cryptic donor site was used and exon 11 was "redefined" through addition of 60 nt derived from intron 11, the transcripts from the mutant allele were processed at about the same rate as the transcripts from the normal allele (fig. 5*B* and 5*C*).

In the region from intron 23 to intron 25, the predominant splice pathway for control cells removed introns 23, 24, and 25 in a processive fashion—intron 23 was removed before intron 24, and intron 25 was excised last (figs. 7*A*–7*C* and 8). In the nuclear cDNA from P1, the use of primers annealing to exon 23 and intron 24 yielded a major product from which intron 23 had been removed (figs. 7*A* and 8), a product that was significantly more abundant in P1 than in control cells at all time points. The intron 24 splice donor site mutation nearly abolished passage of mutant transcripts through the "intron-24-before-intron-25" pathway, and, in contrast with the control individual, there appeared to be a new pathway in which intron 25 was removed prior to intron 24 (fig. 7*C*). Once introns 23 and 25 were excised from the mutant allele, the mutant intron 24 either was removed using a suboptimal cryptic donor site (AG*GTCCTG*) at nt −8 of exon 24 or was retained in a small proportion of mutant transcript (fig. 8). The intron 24 retention product was only detectable in very low abundance in nuclear RNA and had not been seen after amplification of cDNA from total cellular RNA (fig. 2*A*). In a small number of transcripts from the mutant allele, the removal of introns 24 and 25 followed the order that represented the predominant pathway for

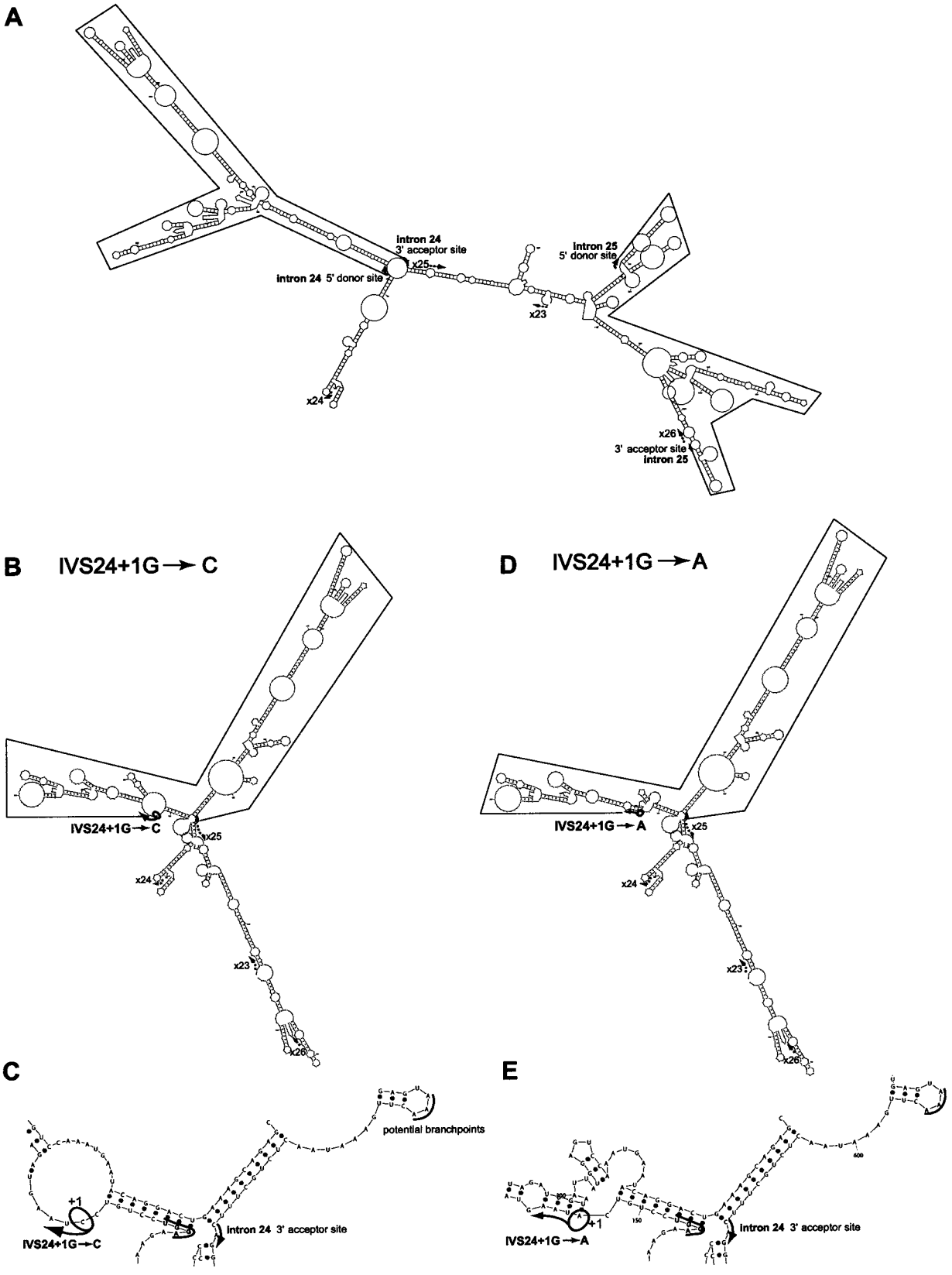
A
Intron 24
3' acceptor site
x25
Intron 24 5' donor site
Intron 25
5' donor site
x23
x24
x26
3' acceptor site
Intron 25
B IVS24+1G→C
IVS24+1G→C
x25
x24
x23
x26
D IVS24+1G→A
IVS24+1G→A
x25
x24
x23
x26
C
potential branchpoints
+1
IVS24+1G→C
Intron 24 3' acceptor site
E
+1
IVS24+1G→A
Intron 24 3' acceptor site

the control individual. That is, when primers were placed in exon 24 and intron 25, a shorter-than-normal splice intermediate was seen, because of removal of intron 25 after intron 24 was removed via use of the cryptic exon 24 donor site (figs. 7*B* and 8).

Transcripts from the mutant allele used the cryptic splice donor site in exon 24, even though its score (59.4) was as low as that for the mutant constitutive intron 24 donor site (60.4)—on the basis of the Shapiro-Senapathy calculation (Shapiro and Senapathy 1987)—presumably because it contained the obligate GT dinucleotide.

RNA Secondary Structure Prediction and Potential Effect on Splice Site Choice

As a first step for examination of a role of mRNA folding in directing use of splice sites, we studied the region of the partially spliced *COL1A2* pre-mRNA extending from exons 23 to 26. We used the mfold program (see the "Material and Methods" section) to obtain information on potential RNA secondary structures and to determine if spatial arrangement might confer an advantage to a cryptic donor site.

We analyzed the RNA of the normal allele that contained exons 23–26 and introns 24 and 25. In 3 of a total of 35 folded structures, the donor and acceptor sites of intron 24 remained single stranded and were brought into juxtaposition, whereas the donor and acceptor sites of intron 25 were located far apart (fig. 9*A*). This structure might facilitate removal of intron 24 prior to excision of intron 25, consistent with the data obtained experimentally (figs. 7 and 8). The donor and acceptor sites were not juxtaposed in the remaining 32 structures.

We then analyzed the mRNAs that contained the mutant sequences (IVS24+1G→C or IVS24+1G→A), using the sequences of exons 23–26 and intron 24 (fig. 9*B* and 9*D*). This splice intermediate is the major intermediate that occurs with excision of intron 25 before use of the cryptic donor site at nt −8 of exon 24 (figs. 7 and 8). The presence of either donor site mutation resulted in juxtaposition of the cryptic donor site and the single-stranded intron 24 acceptor site in 1 of 13 folded structures (fig. 9*C* and 9*E*). None of the other 12 placed the sites in proximity. In 12 folded structures obtained with the wild-type sequence (not shown), the cryptic donor site was always engaged in basepairing interaction and was not situated directly across from the acceptor site. It is conceivable that the spatial proximity between cryptic donor site and acceptor site, caused by either donor-site mutation, promotes spliceosome access and cryptic splice site use.

Discussion

Splice site mutations in the *COL1A2* gene are usually associated with an OI phenotype, the severity of which depends on the location of the mutation. Those near the 3′ end of the coding region of the triple helix are often lethal, whereas those farther 5′ may have a variable phenotype. For example, splice donor site mutations in introns 9 (IVS9+1G→T), 12 (IVS12+1_+19 del), 14 (IVS14+2T→C or →A), and 21 (IVS21+5G→A) lead to exon skipping and moderate OI phenotypes, whereas similar mutations in introns 30 (IVS30+1G→A), 32 (IVS32+1G→A), and 37 (IVS37+1G→T) lead to exon skipping and lethal phenotypes (Byers and Cole 2002). In the individuals we identified in this study, splice donor site mutations result in unstable mRNAs, absence of proα2(I) chain synthesis, and a moderately severe classic EDS phenotype with cardiac valvular involvement. The phenotype is also seen with in-frame nonsense mutations.

Prediction of the effects of splice site mutations on the basis of sequence studies alone is not easy, and several factors may influence the outcome. The "exon-definition" model of splice site pairing suggests that mutations in donor splice sites will result in exon skipping or the activation of cryptic donor sites in the upstream exon, whereas the "intron-definition" model predicts that introns will be retained or cryptic donor sites in the affected intron will be used (Robberson et al. 1990; Berget 1995). These models assume that intron removal follows only one of these pathways, so that complex or mixed outcomes—for example, exon skipping in one population and intron retention in another population of mRNAs derived from the same mutant allele—would not ensue.

In the analysis of splice site mutations in the complex collagen genes, we found that mixed outcomes were common and that determination of the order of intron removal in the local domain helped to predict the products that resulted from splice site mutations (Schwarze

Figure 9 Prediction of secondary structures of *COL1A2* splice intermediates, as shown by mfold. *A,* Normal allele. The folded sequence extends from exons 23 to 26 and contains introns 24 and 25. The intron 24–donor and –acceptor sites are juxtaposed and single stranded, whereas the intron 25 sites are located some distance apart. *B* and *C, IVS24+1G→C,* The folded sequence contains exons 23–26 and intron 24. The site of the mutation at +1 is indicated by an oval attached to an arrow. The enlarged image (*C*) shows that the cryptic donor site at nt −8 in exon 24, highlighted by a thick line, is juxtaposed to the single-stranded acceptor site of intron 24. Potential branchpoints are shown. *D* and *E, IVS24+1G→A,* Folding results are shown, as in panels B and C. Intron sequences are framed by thin lines (*A, B,* and *D*). The beginning of exon sequences is indicated by dashed arrows (*A, B,* and *D*). Donor and acceptor sites are indicated by solid arrows.

et al. 1999; Takahara et al. 2002). In this fashion, mutations in rapidly removed introns generally led to exon skipping, whereas those in slowly removed introns led to intron inclusion or use of cryptic sites. As noted by Kessler and colleagues for the genes they studied (Kessler et al. 1993), we found that some introns in collagen genes appeared to participate in more than one pathway and so were sometimes "fast" and sometimes "slow." "Fast" and "slow" in this context are defined with respect to relative rate of removal of adjacent introns and also imply an "independent" or "dependent" character of removal, in that "slow" intron removal reflects the need for prior removal of "fast" introns.

In three of the six mutant alleles we identified in the *COL1A2* gene in this study, donor splice site alterations led to mRNA instability. In two of the others, the same nonsense codon resulted in mRNA instability, whereas, in the sixth, the inclusion of a cryptic exon that contained multiple termination codons had the same effect. At first glance, the splice donor mutations (IVS11+5G→A, IVS24+1G→A, and IVS24+1G→C) are similar to those that in other introns produce exon skipping and a stable mRNA. In each current instance, however, the result is an unstable mRNA. We think this is best explained by the order in which introns are normally removed.

In control cells, the removal of intron 24 follows removal of intron 23, so that skipping of exon 24 would not be possible in the presence of a donor site mutation in intron 24. Following this prediction, in the cells that contain the IVS24 mutations, intron 24 is retained for an extended period, a suboptimal cryptic donor site that creates a translational frameshift is used, and the mRNA is rapidly degraded.

Prediction of the outcome of the mutation in intron 11 is modified by the presence of a strong cryptic donor site 61 nt downstream from the constitutive site. In this domain, intron 11 is ordinarily removed in two pathways. In one pathway, intron 10 is removed prior to intron 11; in the other, the order is reversed. In the pathway in which intron 10 is removed quickly, exon skipping is not available to resolve the splicing in the presence of the intron 11 splice donor site mutation, and so the use of a cryptic site follows. However, in the pathway in which intron 11 would be removed rapidly, exon skipping is expected, but, in all instances, the near optimal cryptic donor site is used. One explanation for this outcome appears to be a long delay in removal of intron 11 that permits redirection of splicing for many transcripts, such that intron 10 is removed rapidly. As a consequence, it appears that the majority of transcripts may be shuttled through the intron 10 "first" pathway, so that ultimately, the only choice of donor sites in intron 11 is the near-optimal cryptic site. Such redirection might reflect refolding of the nascent transcript to permit spliceosome access (see, e.g., Howe and Ares [1997]).

Intron removal is thought to be largely cotranscriptional, although evidence for this concept is not available for many genes (Neugebauer and Roth 1997; Goldstrohm et al. 2001; Bentley 2002). Indeed, for *COL1A1,* at least one intron appears to be retained for a considerable time following transcription (Johnson et al. 2000). Support for the idea that removal of introns is not processive—that is, does not occur in the order of transcription—is derived largely from the types of studies described here, albeit in smaller genes (Lang et al. 1985; Lang and Spritz 1987; Gudas et al. 1990; Kessler et al. 1993). One concern about those studies and the present study is that the substrate studied is not well defined. That is, is the population of mRNAs studied simply a splicing "backwater" in which abnormally spliced transcripts accumulate? At this point, there are data neither to support nor to refute such a notion. The idea that the order of intron removal can predict, in part, the outcome of mutations at splice sites is supported by our studies of several collagen genes (*COL1A1, COL1A2, COL3A1,* and *COL5A1*) (Schwarze et al. 1999; Takahara et al. 2002; U.S. unpublished data) and by those in the fibrinogen α gene (*FGA*) (Attanasio et al. 2003). The mechanisms by which splice order is determined are not clear but could include both folding of the nascent transcript (Balvay et al. 1993; Howe and Ares 1997) and transcriptional pausing (Keene et al. 1999), which can augment upstream splicing.

In one other patient with this type of EDS in whom no proα2(I) chains could be detected, a splice donor site mutation in intron 46 was identified (IVS46+2T→C). This mutation permitted almost exclusive use of a cryptic donor site 17 nt upstream in the exon (Nicholls et al. 2001), but a very small amount of normal transcript was detected. It is surprising that this patient had features of OI, suggesting that abnormal protein chains were made. Although the published studies did not identify an exon-skip product that might explain the phenotype, such a product could derive from a low-abundance alternative pathway that was not appreciated.

This form of EDS and a moderately severe recessively inherited form of OI (Nicholls et al. 1979) share apparent similarities in their biochemical phenotype, in that cells from affected individuals appear to synthesize no proα2(I) chains. The mutations underlying the two phenotypes are different. In this form of EDS, the mRNA from the mutant alleles is unstable, and mRNA degradation probably occurs in the nucleus or related to a first round of translation, so that no abnormal protein is synthesized. In contrast, the moderately severe OI type III phenotype results from homozygosity for a short deletion and frameshift near the end of the coding

region of the mRNA (Pihlajaniemi et al. 1984). The mRNA is stable, but the proα2(I) polypeptide chain fails to fold normally and is unstable and degraded. The basis for OI in that patient is not clear but may result from synthesis of a small number of abnormal molecules that contain the defective chain. A similar phenotype is seen in the *oim/oim* mouse with a virtually identical mutation (Chipman et al. 1993). There is no follow-up information published about the child with this form of OI, so we cannot exclude the possibility that he has a valvular phenotype. The *oim/oim* mouse does not appear to have a valvular phenotype.

The phenotype of these individuals with "pure" *COL1A2* nulls includes valvular heart disease. Two of the four adults described here had involvement of both the aortic and mitral valves (P1 and P3), and in the other two either the aortic valve (brother of P3) or the mitral valve (P2) was involved. All four individuals underwent valve replacement surgery, as did the fifth patient, with aortic valve involvement, described by Sasaki et al. (1987). The sixth known patient is a child and so is still potentially at risk (Nicholls et al. 2001). These findings suggest that the α2(I) chain is important for functions in soft tissues but that bone can form in a normal or near-normal fashion in individuals whose cells make no α2(I) chains. This is an unexpected finding of the study of these mutations, one that warrants more detailed investigation into the function of the chain in different tissues.

Acknowledgments

This work was supported, in part, by National Institutes of Health grants AR41223 and AR21557.

Electronic-Database Information

The URL for data presented herein is as follows:

Online Mendelian Inheritance in Man (OMIM), http://www.ncbi.nlm.nih.gov/Omim/ (for EDS, *TNXB,* and type I procollagen)

References

Attanasio C, David A, Neerman-Arbez M (2003) Outcome of donor splice site mutations accounting for congenital afibrinogenemia reflects order of intron removal in the fibrinogen α gene (FGA). Blood 101:1851–1856

Balvay L, Libri D, Fiszman MY (1993) Pre-mRNA secondary structure and the regulation of splicing. Bioessays 15:165–169

Bentley D (2002) The mRNA assembly line: transcription and processing machines in the same factory. Curr Opin Cell Biol 14:336–342

Berget SM (1995) Exon recognition in vertebrate splicing. J Biol Chem 270:2411–2414

Bonadio J, Holbrook KA, Gelinas RE, Jacob J, Byers PH (1985) Altered triple helical structure of type I procollagen in lethal perinatal osteogenesis imperfecta. J Biol Chem 260:1734–1742

Bouma P, Cabral WA, Cole WG, Marini JC (2001) COL5A1 exon 14 splice acceptor mutation causes a functional null allele, haploinsufficiency of α 1(V) and abnormal heterotypic interstitial fibrils in Ehlers-Danlos syndrome II. J Biol Chem 276:13356–13364

Burch GH, Gong Y, Liu W, Dettman RW, Curry CJ, Smith L, Miller WL, Bristow J (1997) Tenascin-X deficiency is associated with Ehlers-Danlos syndrome. Nat Genet 17:104–108

Byers PH, Cole WG (2002) Osteogenesis imperfecta. In: Royce PM, Steinmann B (eds) Connective tissue and its heritable disorders: molecular, genetic and medical aspects. Wiley-Liss, New York, pp 385–430

Chipman SD, Sweet HO, McBride DJ Jr, Davisson MT, Marks SC Jr, Shuldiner AR, Wenstrup RJ, Rowe DW, Shapiro JR (1993) Defective pro α 2(I) collagen synthesis in a recessive mutation in mice: a model of human osteogenesis imperfecta. Proc Natl Acad Sci USA 90:1701–1705

De Paepe A, Nuytinck L, Hausser I, Anton-Lamprecht I, Naeyaert JM (1997) Mutations in the COL5A1 gene are causal in the Ehlers-Danlos syndromes I and II. Am J Hum Genet 60:547–554

Giunta C, Steinmann B (2000) Compound heterozygosity for a disease-causing G1489E [correction of G1489D] and disease-modifying G530S substitution in COL5A1 of a patient with the classical type of Ehlers-Danlos syndrome: an explanation of intrafamilial variability? Am J Med Genet 90: 72–79

Goldstrohm AC, Greenleaf AL, Garcia-Blanco MA (2001) Co-transcriptional splicing of pre-messenger RNAs: considerations for the mechanism of alternative splicing. Gene 277: 31–47

Gudas JM, Knight GB, Pardee AB (1990) Ordered splicing of thymidine kinase pre-mRNA during the S phase of the cell cycle. Mol Cell Biol 10:5591–5595

Hata R, Kurata S, Shinkai H (1988) Existence of malfunctioning pro α 2(I) collagen genes in a patient with a pro α 2(I)-chain-defective variant of Ehlers-Danlos syndrome. Eur J Biochem 174:231–237

Howe KJ, Ares M Jr (1997) Intron self-complementarity enforces exon inclusion in a yeast pre-mRNA. Proc Natl Acad Sci USA 94:12467–12472

Johnson C, Primorac D, McKinstry M, McNeil J, Rowe D, Lawrence JB (2000) Tracking COL1A1 RNA in osteogenesis imperfecta: splice-defective transcripts initiate transport from the gene but are retained within the SC35 domain. J Cell Biol 150:417–432

Keene RG, Mueller A, Landick R, London L (1999) Transcriptional pause, arrest and termination sites for RNA polymerase II in mammalian N- and c-myc genes. Nucleic Acids Res 27: 3173–3182

Kessler O, Jiang Y, Chasin LA (1993) Order of intron removal during splicing of endogenous adenine phosphoribosyltransferase and dihydrofolate reductase pre-mRNA. Mol Cell Biol 13:6211–6222

Kojima T, Shinkai H, Fujita M, Morita E, Okamoto S (1988)

Case report and study of collagen metabolism in Ehlers-Danlos syndrome type II. J Dermatol 15:155–160

Lang KM, Spritz RA (1987) In vitro splicing pathways of pre-mRNAs containing multiple intervening sequences? Mol Cell Biol 7:3428–3437

Lang KM, van Santen VL, Spritz RA (1985) The two intervening sequences of human β- and γ-globin pre-mRNAs are excised in a preferred temporal order in vitro. EMBO J 4: 1991–1996

Maquat LE, Carmichael GG (2001) Quality control of mRNA function. Cell 104:173–176

Michalickova K, Susic M, Willing MC, Wenstrup RJ, Cole WG (1998) Mutations of the α 2(V) chain of type V collagen impair matrix assembly and produce Ehlers-Danlos syndrome type I. Hum Mol Genet 7:249–255

Neugebauer KM, Roth MB (1997) Transcription units as RNA processing units. Genes Dev 11:3279–3285

Nicholls AC, Oliver JE, McCarron S, Harrison JB, Greenspan DS, Pope FM (1996) An exon skipping mutation of a type V collagen gene (COL5A1) in Ehlers-Danlos syndrome. J Med Genet 33:940–946

Nicholls AC, Pope FM, Schloon H (1979) Biochemical heterogeneity of osteogenesis imperfecta: new variant. Lancet 1: 1193

Nicholls AC, Valler D, Wallis S, Pope FM (2001) Homozygosity for a splice site mutation of the COL1A2 gene yields a non-functional pro(α)2(I) chain and an EDS/OI clinical phenotype. J Med Genet 38:132–136

Nuytinck L, Freund M, Lagae L, Pierard GE, Hermanns-Le T, De Paepe A (2000) Classical Ehlers-Danlos syndrome caused by a mutation in type I collagen. Am J Hum Genet 66:1398–1402

Pihlajaniemi T, Dickson LA, Pope FM, Korhonen VR, Nicholls A, Prockop DJ, Myers JC (1984) Osteogenesis imperfecta: cloning of a pro-α 2(I) collagen gene with a frameshift mutation. J Biol Chem 259:12941–12944

Richards AJ, Martin S, Nicholls AC, Harrison JB, Pope FM, Burrows NP (1998) A single base mutation in COL5A2 causes Ehlers-Danlos syndrome type II. J Med Genet 35:846–848

Robberson BL, Cote GJ, Berget SM (1990) Exon definition may facilitate splice site selection in RNAs with multiple exons. Mol Cell Biol 10:84–94

Sasaki T, Arai K, Ono M, Yamaguchi T, Furuta S, Nagai Y (1987) Ehlers-Danlos syndrome: a variant characterized by the deficiency of pro α 2 chain of type I procollagen. Arch Dermatol 123:76–79

Schalkwijk J, Zweers MC, Steijlen PM, Dean WB, Taylor G, van Vlijmen IM, van Haren B, Miller WL, Bristow J (2001) A recessive form of the Ehlers-Danlos syndrome caused by tenascin-X deficiency. N Engl J Med 345:1167–1175

Schwarze U, Atkinson M, Hoffman GG, Greenspan DS, Byers PH (2000) Null alleles of the *COL5A1* gene of type V collagen are a cause of the classical forms of Ehlers-Danlos syndrome (types I and II). Am J Hum Genet 66:1757–1765

Schwarze U, Starman BJ, Byers PH (1999) Redefinition of exon 7 in the *COL1A1* gene of type I collagen by an intron 8 splice-donor–site mutation in a form of osteogenesis imperfecta: influence of intron splice order on outcome of splice-site mutation. Am J Hum Genet 65:336–344

Shapiro MB, Senapathy P (1987) RNA splice junctions of different classes of eukaryotes: sequence statistics and functional implications in gene expression. Nucleic Acids Res 15:7155–7174

Takahara K, Schwarze U, Imamura Y, Hoffman GG, Toriello H, Smith LT, Byers PH, Greenspan DS (2002) Order of intron removal influences multiple splice outcomes, including a two-exon skip, in a *COL5A1* acceptor-site mutation that results in abnormal pro-α1(V) N-propeptides and Ehlers-Danlos syndrome type I. Am J Hum Genet 71:451–465

Vogel A, Holbrook KA, Steinmann B, Gitzelmann R, Byers PH (1979) Abnormal collagen fibril structure in the gravis form (type I) of Ehlers-Danlos syndrome. Lab Invest 40:201–206

Wenstrup RJ, Florer JB, Willing MC, Giunta C, Steinmann B, Young F, Susic M, Cole WG (2000) COL5A1 haploinsufficiency is a common molecular mechanism underlying the classical form of EDS. Am J Hum Genet 66:1766–1776

Wenstrup RJ, Langland GT, Willing MC, D'Souza VN, Cole WG (1996) A splice-junction mutation in the region of COL5A1 that codes for the carboxyl propeptide of pro α 1(V) chains results in the gravis form of the Ehlers-Danlos syndrome (type I). Hum Mol Genet 5:1733–1736

Zuker M (2003) Mfold Web server for nucleic acid folding and hybridization prediction. Nucleic Acids Res 31:3406–3415